CRITICAL GAS VELOCITY REQUIRED FOR COMPLETE SUSPENSION OF SOLID PARTICLES IN SOLID-SUSPENDED BUBBLE COLUMN WITH DRAUGHT TUBE

KOZO KOIDE, KAZUYOSHI HORIBE, HIROKAZU KAWABATA AND SHIGETAKA ITO

Department of Chemical Engineering, Shizuoka University, Hamamatsu 432

Key Words: Bubble Column, Draught Tube, Solid Particle Suspension, Fluidization, Critical Gas Velocity

The critical gas velocity required for complete suspension of solid particles was studied experimentally in a solid-suspended bubble column with a draught tube. It was shown that the critical gas velocity increases with increasing terminal velocity of a single particle, solid concentration, liquid surface tension, diameter of gas distributor and density difference between solid and liquid, and decreases with increasing column diameter and liquid viscosity.

Based on these observations, an empirical equation for critical gas velocity is proposed that is applicable to columns with diameters of 0.1–0.3 m.

Introduction

The solid-suspended bubble column with a draught tube and a conical bottom (usually with a $\pi/3$ rad angle), often called the pachuca tank, is used widely for leaching ores.[8] In this column the gas is dispersed into the draught tube and a stable circulating liquid flow is induced by apparent density difference between the aerated liquid in the draught tube and that in the annulus. This circulating liquid flow brings settling solids in the conical bottom into the region of the column top. To design a column of this type as a slurry reactor, the values of the critical gas velocity U_c required for complete suspension of solid particles and their concentration distribution should be known. However, only a few research works[9,10] have been reported on U_c. Muroyama *et al.*[10] have proposed an empirical equation for the critical solid holdup, which is defined as the maximum solid amount maintained in complete suspension for a given gas velocity. However, this equation is applicable only to the slurry of water-activated carbon particles, and the effect of liquid and solid properties on the critical solid holdup is not clear.

The purpose of this study is to clarify experimentally the effects of column dimensions and properties of the liquid and the solid particles on the critical gas velocity required for complete suspension of solid particles in the solid-suspended bubble column with draught tube in liquid-solid batch operation.

Received October 21, 1983. Correspondence concerning this article should be addressed to K. Koide. K. Horibe is now with Shin Nihon Seitetsu Co., Ltd., Himeji 671-11.

1. Experimental

The experimental apparatus used in this work is shown in **Fig. 1**. The dimensions of plexiglass columns used are shown in **Table 1**. As shown in **Fig. 2**, the column bottom consists of a conical section with a cone angle of $\pi/3$ rad, and a perforated plate is used as gas distributor. The perforated plate is covered with a stainless steel wire gauze of 260–300 mesh to prevent the solid particles from penetrating to the gas distributor through the holes, and the holes of the gas distributor are oriented in triangular pitches. Table 1 shows the dimensions of draught tubes and the vertical clearance L between the lower end of the draught tube and the wall of the conical bottom shown in Fig. 2. **Table 2** shows details of the gas distributors.

The liquids used in this work were demineralized water and aqueous solutions of glycerol and glycol, and the gas used was air. The values of the static slurry height H_L above the gas distributor are shown in Table 1. The operating temperature was kept at 298.2 ± 0.5 K. **Table 3** shows the physical properties of liquids, and **Table 4** shows those of glass and bronze spheres. The particle diameter d_p in the latter table is the median diameter obtained from the weight cumulative particle size distribution. The terminal velocity V_t of a single particle in stagnant liquid was calculated on the basis of d_p values listed in Table 3. The concentration of solid particles was varied in the range of 25–400 $kg \cdot m^{-3}$.

Two different methods were employed to determine

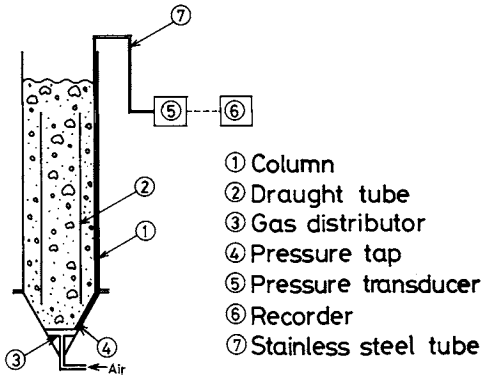

Fig. 1. Experimental apparatus.

Table 1. Experimental apparatus

D_o [m]	D_i* [m]	H [m]	H_L [m]	$L\times10^2$ [m]	Perforated plate**
0.100	0.060	1.40	1.50	2.1	P1, P2
0.140	0.066	1.40	1.54	3.0	P1
0.140	0.082	0.70–2.10	0.84–2.24	1.2–7.1	P1, P2, P3
0.140	0.094	1.40	1.54	3.0	P1
0.140	0.104	1.40	1.54	3.0	P1
0.218	0.128	1.40	1.58	4.8	P4, P5
0.300	0.190	1.40	1.68	6.2	P4, P5, P6

* $t_w=3$ mm for $D_i\leqq0.128$ m and 5 mm for $D_i=0.190$ m.
** Dimensions of perforated plates are shown in Table 2.

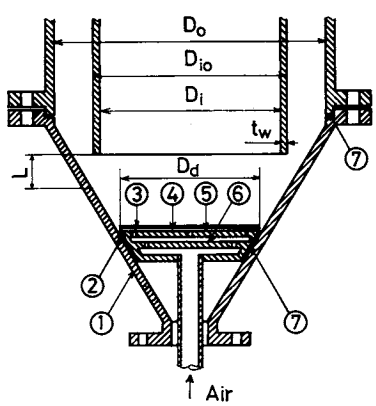

Fig. 2. Details of gas distributor. 1, conical bottom; 2, gas distributor; 3, stainless steel rim; 4, stainless steel guaze; 5, perforated plate; 6, buffer plate; 7, rubber packing.

Table 2. Dimensions of perforated plates

Gas distributor	D_d [m]	δ [mm]	n [—]
P1	0.035	3	3
P2	0.050	3	7
P3	0.070	3	7
P4	0.054	4	7
P5	0.086	3	10
P6	0.150	2	38

the critical gas velocity U_c required for complete suspension of solid particles: pressure drop measurement and visual observation. Solid particles of known

Table 3. Properties of solid particles

Materials	Size [mesh]	d_p [μm]	$V_t\times10^2$ [m·s^{-1}]
Glass sphere	24–35	498	7.79 (in water)
$\rho_p=2500$ kg·m^{-3}	60–80	198	2.44 (in water)
	60–80	198	0.990 (in 39GL*)
	60–80	198	0.472 (in 55GL*)
	60–80	198	0.185 (in 69GL*)
	60–80	198	0.635 (in 71EG*)
	60–80	198	0.548 (in 73EG*)
	80–100	136	1.40 (in water)
	100–140	117	1.09 (in water)
High index Glass sphere	140–200	79.0	1.25 (in water)
$\rho_p=4680$ kg·m^{-3}			
Bronze sphere	140–200	89.0	2.91 (in water)
$\rho_p=8770$ kg·m^{-3}			

* 39GL, 55GL and 69GL: 39.4, 55.2 and 68.6 wt% glycerol aq. solns. 71EG and 73EG: 70.5 and 72.9 wt% ethylene glycol aq. solns.

Table 4. Properties of liquids at 298.2 K

Liquid	ρ [kg·m^{-3}]	$\mu\times10^3$ [Pa·s]	$\sigma\times10^3$ [N·m^{-1}]
Water	997.0	0.894	72.0
39.4 wt% Glycerol aq. soln	1098	2.81	69.7
55.2 wt% Glycerol aq. soln	1142	6.13	67.6
68.6 wt% Glycerol aq. soln	1178	15.2	65.0
75.5 wt% Ethylene glycol aq. soln	1085	4.76	53.5
72.9 wt% Ethylene glycol aq. soln	1088	5.50	51.7

quantity were settled in the liquid at a constant temperature to adjust the static slurry height to a certain value, and then air was dispersed into the column through the gas distributor with sufficient gas velocity to suspend all solid particles. Then, as gas velocity was gradually decreased, the total pressure drop ΔP_s due to the suspended solid in the liquid was measured with a pressure transducer connected to a Prandtl tube located at the same level as the gas distributor, where the output signal from the pressure transducer was adjusted to indicate zero value at $U_G=0$. Simultaneously, the behavior of solid particles over the gas distributor was observed visually.

2. Results and Discussion

2.1 Determination of U_c

Figure 3 shows the relationship between ΔP_s and the gas velocity based on the cross section of the column. For U_G greater than a certain value, ΔP_s becomes almost constant. In this region designated as A in Fig. 3, solid particles are all in suspension and circulating liquid flow in the column as shown in **Fig. 4**(a). Solid particles which tend to settle along the conical wall are picked up by the local circulating

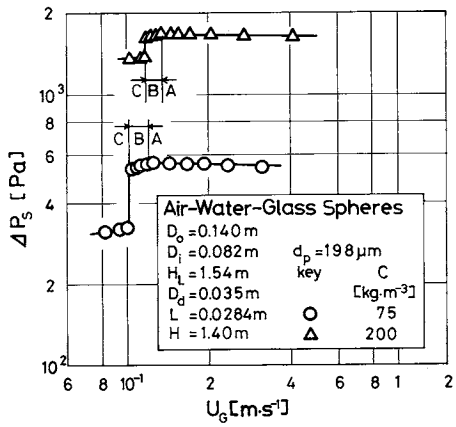

Fig. 3. Pressure drop vs. gas velocity curves.

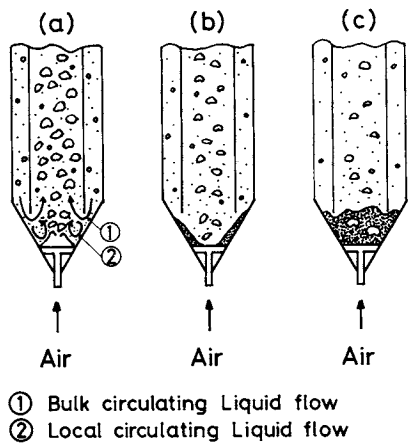

Fig. 4. Phase transition with decreasing gas velocity.

liquid flow induced by gas flow from the gas distributor and then carried upwards by the bulk circulating liquid flow induced by the difference between gas holdup in the draught tube and that in the annulus. As U_G was gradually decreased, clouds with high solid concentration were generated, and a small part of the solid particles began to stay on the periphery of the gas distributor as shown in Fig. 4(b). This phenomenon was observed at U_G in region B in Fig. 3. Decreasing U_G further resulted in a situation where most solid particles settled down on the gas distributor to form a mobile packed bed as shown in Fig. 4(c). When the height of this bed was higher than the level of the lower end of the draught tube, the bulk circulating liquid flow ceased. These situations were observed in region C in Fig. 3.

Three straight lines corresponding to the three regions of U_G were obtained in the $\log \Delta P_s$ vs. $\log U_G$ plot as shown in Fig. 3. The gas velocity at the transition point from region A to region B agreed with the lowest gas velocity where all the particles were observed to be in suspension. Therefore, the critical gas velocity U_c required for complete suspension of solid particles was determined as the transition point from region A to region B in Fig. 3.

2.2 Effect of liquid and solid properties on U_c

Figure 5 shows that U_c is roughly proportional to $V_t^{1.1}$. **Figure 6** shows that U_c increases slightly with increasing solid concentration c, to be proportional to $c^{0.27}$. **Figure 7** shows that U_c increases with increasing density difference between the solid particle and the liquid, and $U_c/V_t^{1.1}$ is roughly proportional to $\{(\rho_p-\rho)/\rho\}^{0.75}$.

To see the effect of liquid viscosity μ on U_c, $(U_c/V_t^{1.1})(c/\rho_p)^{0.27}\{(\rho_p-\rho)/\rho\}^{0.75}$ is plotted against μ as shown in **Fig. 8**. Values for the quantity taken in the ordinate are almost constant for values of μ lower than 0.003Pa·s, but increase with increasing μ in the range of μ higher than 0.003Pa·s. This figure does not show the effect of μ on U_c explicitly, but since V_t decreases with increasing μ, e.g., $V_t \propto \mu^{-1}$ in the Stokes' law region, it can be said that U_c decreases with increasing μ.

2.3 Effect of column dimensions on U_c

Figure 9 shows that the ratio of flow path area ($\pi D_{io} L$) under the lower end of the draught tube (see Fig. 2) and the cross-sectional area ($\pi D_o^2/4$) of the column has no effect on U_c in the range of this ratio larger than about 0.4, while U_c decreases with decreasing area ratio in the range of this ratio smaller than about 0.4. This phenomenon might be due to the fact that the bulk circulating liquid flow penetrates into the column bottom as the area ratio decreases, and then the settling particles near the base plate of the column are picked up by this liquid flow directly.

Figure 10 shows that U_c has a minimum value at a certain value of draught tube length H. Average velocity U_{LC} of the bulk circulating liquid flow is roughly proportional to $H^{1/2}$ in a bubble column with draught tube,[2] and the increase in U_{LC} might cause U_c to decrease. On the other hand, the total weight of the solid particles to be suspended is proportional to H_L (roughly to H in this work) for constant value of c, and the increase in total weight of solid particles might cause U_c to increase. The dependence of U_c on H shown in Fig. 10 might be attributed to these conflicting effects of H on the mechanism of suspending solid particles.

Figure 11 shows that a reduction of U_c value can be achieved by using a conical bottom with small value for D_d/D_o. This figure shows also that the degree of reduction of U_c value with decreasing D_d/D_o is higher for the liquid of lower surface tension. **Figure 12** shows that when column diameter is increased, the degree of reduction of U_c value with decreasing D_d/D_o becomes higher and the value for U_c at a given value of D_d/D_o becomes lower. Since reviewing previous works[1-3,7,9] on U_{LC} in bubble columns with draught tube indicates that U_{LC} is almost constant for different

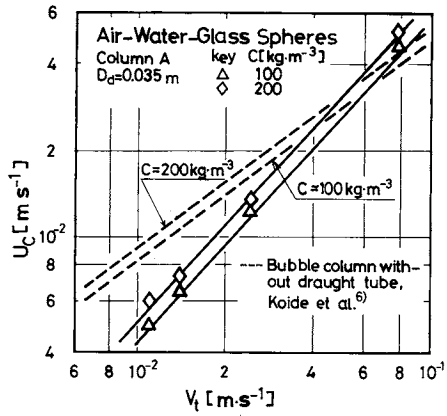

Fig. 5. Effect of terminal velocity of a single particle on U_c. Column A: $D_o=0.14$ m; $D_i=0.082$ m; $H=1.40$ m; $H_L=1.54$ m; $L=0.030$ m.

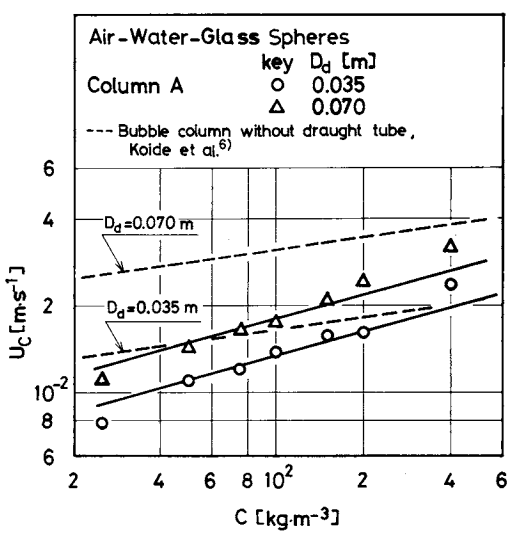

Fig. 6. Effect of solid concentration on U_c. $d_p=198$ μm.

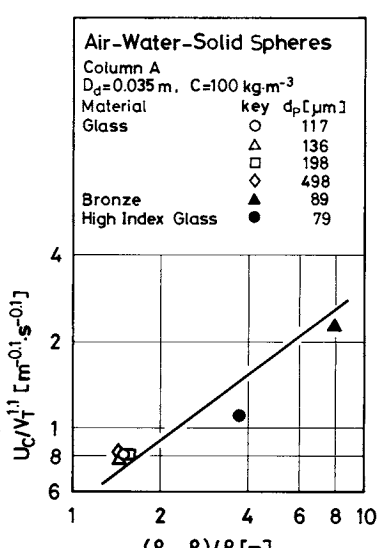

Fig. 7. Effect of density difference between solid and liquid on $U_c/V_t^{1.1}$.

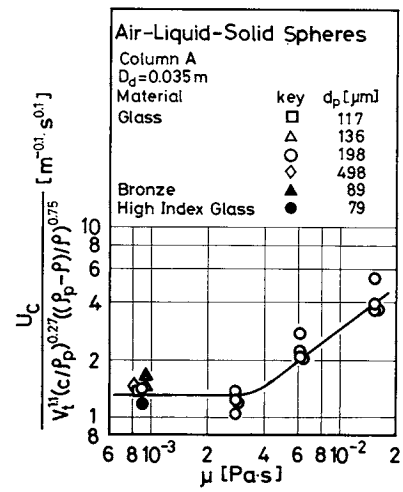

Fig. 8. Preliminary correlation of U_c.

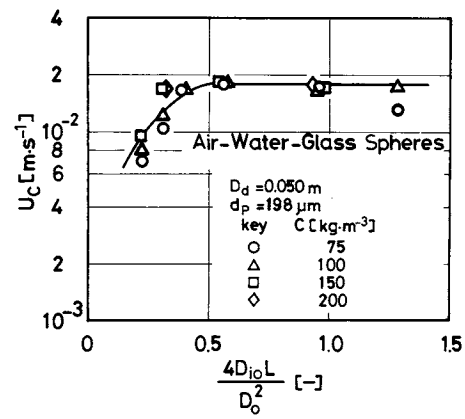

Fig. 9. Effect of flow path area under lower end of draught tube. $D_o=0.14$ m; $D_{io}=0.088$ m; $H=1.40$ m.

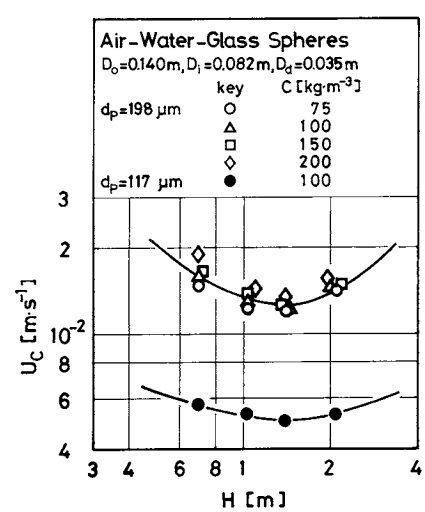

Fig. 10. Effect of draught tube length on U_c.

values of D_o, the reduction of U_c with increasing D_o might be due not to the increase in U_{LC} but to increasing turbulent motion of liquid near the conical bottom with increasing D_o.

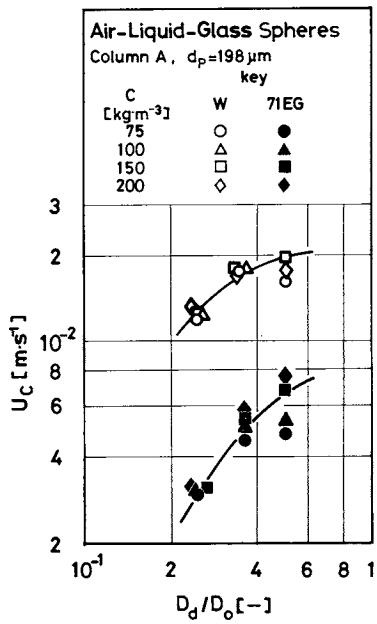

Fig. 11. Effect of shape of conical bottom and liquid properties on U_c.

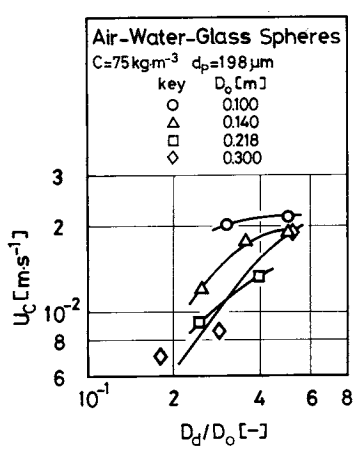

Fig. 12. Effect of shape of conical bottom and column diameter on U_c.

Figure 13 shows that U_c has a minimum value at $D_i/D_o \simeq 0.6$ for each constant value of c larger than $100\,\mathrm{kg\cdot m^{-3}}$. Since U_{LC} shows a maximum value at $D_i/D_o \simeq 0.6$ in the bubble column without solid particles,[7] a similar phenomenon might occur in the column used in this work, and then U_c shows a minimum value at $D_i/D_o \simeq 0.6$. However, at $c = 75\,\mathrm{kg\cdot m^{-3}}$ U_c decreases slightly with increasing D_i/D_o. The bulk circulating liquid flow from the annulus into the draught tube carries upwards the solid particles which are picked up from the conical bottom by the local circulating liquid flow, and plays a role in reducing the solid concentration in the conical bottom. Since U_{LC} for different D_i/D_o might be large enough for the bulk circulating liquid flow to carry upwards the solid particles at $c = 75\,\mathrm{kg\cdot m^{-3}}$, the process whereby the solid particles are picked up by

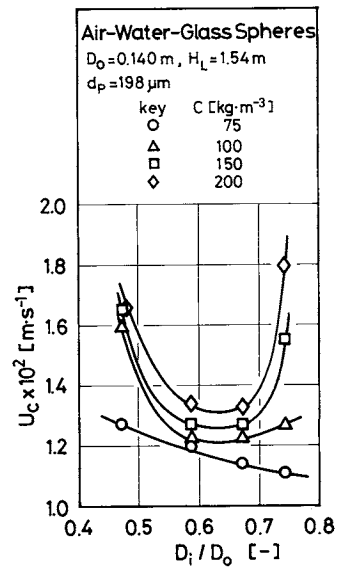

Fig. 13. Effect of inner diameter of draught tube on U_c.

the local circulating liquid flow might be the controlling step for suspending the solid particles. Therefore, the effect of D_i/D_o on U_c is not so large at $c = 75\,\mathrm{kg\cdot m^{-3}}$.

2.4 Correlation of U_c

The observations above show that for the column A of $D_d = 0.035\,\mathrm{m}$

$$U_c/[V_t^{1.1}(c/\rho_p)^{0.27}\{(\rho_p-\rho)/\rho\}^{0.75}]$$

depends on μ, but for the columns other than column A the relation of $U_c \propto V_t^{1.1}$ does not necessarily hold. Therefore, an equation in the form of Eq. (1) was assumed to express the effects of liquid and solid properties and column dimensions on U_c for $(4D_{io}L/D_o^2) > 0.4$, where the effects of D_i/D_o, H and D_d/D_o on U_c, respectively, were expressed by the terms S_o/S_a and S_o/S_i, the second bracketed term and the last one.* The numerical constants in Eq. (1) were decided by the direct search method[4] using data observed in this work,

$$\frac{U_c}{V_t} = 4.60\left(\frac{c}{\rho_p}\right)^{0.273}\left(\frac{\rho_p-\rho}{\rho}\right)^{0.750}\left(\frac{V_t\mu}{\sigma}\right)^{-0.634} \times\left(\frac{D_o^2 g\rho}{\sigma}\right)^{-0.340}\left(\frac{S_o}{S_a}\right)^{0.546}\left(\frac{S_o}{S_i}\right)^{0.454} \times\left\{1+897\left(\frac{g\mu^4}{\rho\sigma^3}\right)^{0.290}\right\} \times\left\{\left(\frac{V_t}{\sqrt{gH}}\right)+1.47\times10^{-4}\left(\frac{H}{D_o}\right)\right\} \times\left\{1-1.32\left(1-\frac{D_d}{D_o}\right)^{0.997(D_o^2 g\rho/\sigma)^{0.172}}\right\} \quad (1)$$

* The functional form in the last brackets in Eq. (1) to express the effect of D_d/D_o is similar to that used in the previous paper.[6]

in the experimental ranges of $8.55 \leqq (c/\rho_p) \leqq 0.160$,
$1.12 \leqq \{(\rho_p - \rho)/\rho\} \leqq 7.80$,
$1.31 \times 10^{-4} \leqq (V_t \mu/\sigma) \leqq 9.67 \times 10^{-4}$,
$1.36 \times 10^{3} \leqq (D_o^2 g \rho/\sigma) \leqq 1.22 \times 10^{4}$,
$1.68 \times 10^{-11} \leqq (g\mu^4/\rho\sigma^3) \leqq 1.62 \times 10^{-6}$,
$0.18 \leqq (D_d/D_o) \leqq 0.5$,
$4.99 \times 10^{-4} \leqq (V_t/\sqrt{gH}) \leqq 2.10 \times 10^{-2}$,
$4.67 \leqq (H/D_o) \leqq 15$,
$0.222 \leqq (S_i/S_o) \leqq 0.552$.

Figure 14 shows that U_c values estimated by Eq. (1) agree relatively well with those observed experimentally, and the average error of estimation was 13% for 142 data.

2.5 Comparison of this work with previous ones

1) Bubble column without draught tube From visual observation solid particles are distributed more uniformly in the column with draught tube than in the column without the tube where the solid concentration decreases exponentially with increasing height from column bottom.[5] Figures 5 and 6 show that values for U_c observed in this work are much smaller than those observed in the column without draught tube.[6] However, when a column with conical bottom of small value for D_d ($D_d = 0.035$ m) is used, the difference between values for U_c observed in the columns with and without draught tube becomes small for a slurry of large particles. The reason might be that the local circulating liquid flow has to pick up large particles on the conical bottom before the bulk circulating liquid carries them upwards, and the former process controls in suspending large particles. Concerning the effects of other column dimensions on U_c, Eq. (1) shows that U_c is roughly proportional to $D_o^{-0.7}$, while $U_c \propto D_o^{0.1}$ and H have no effect on U_c in the column without draught tube.[6]

2) Bubble column with draught tube **Figure 15** shows that agreement of the values of U_c estimated by Eq. (1) with those observed by Muroyama *et al.*[10] for the suspension of activated carbon particles in water is not so good, and the dependence of U_c on solid concentration is much pronounced for the data of Muroyama *et al.* This disagreement might be attributed to the difference in solid density; $(\rho_p - \rho)/\rho \simeq 0.3$ in their work and $1.12 \leqq (\rho_p - \rho)/\rho \leqq 7.80$ in this work.

Matsuura *et al.*[9] measured the critical gas velocity above which solid particles circulated from the draught tube to the annulus, and showed a hysteresis phenomenon whereby the critical gas velocity observed when U_G was gradually increased to circulate the solid particles was larger than that observed when U_G was gradually decreased to cease the circulation of solid particles. As Eq. (1) is based on U_c values observed when U_G is gradually decreased, care should be taken for the hysterisis phenomenon noted above when Eq. (1) is used for estimating the operating

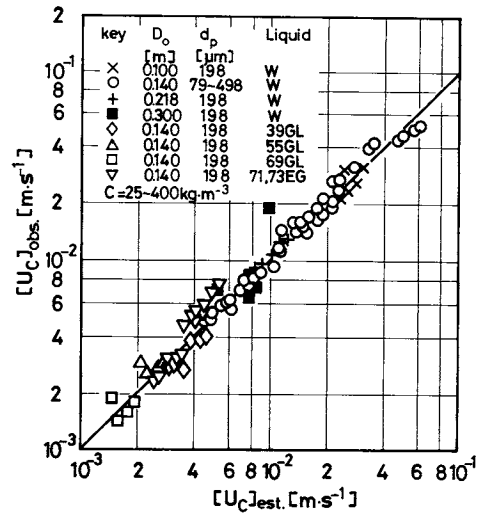

Fig. 14. Comparison of U_c estimated from Eq. (1) with values observed in this work.

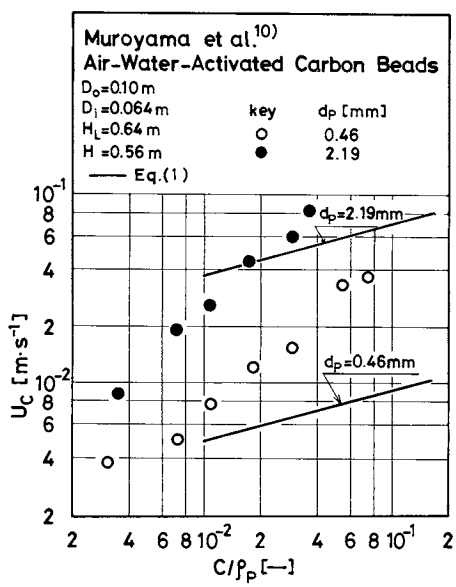

Fig. 15. Comparison of U_c estimated from Eq. (1) with values observed in previous work.

conditions of gas velocity.

To clarify the mechanism of suspending solid particles, further work is necessary on U_{LC} and the solid concentration distribution, as were done by Matsuura *et al.*

Conclusions

1) The critical gas velocity U_c required for complete suspension of solid particles in the solid-suspended bubble column with draught tube and with conical bottom increases with increasing terminal velocity of a single particle, solid particle concentration, diameter of gas distributor and solid density, and decreases with increasing column diameter and liquid viscosity.

2) Solid particles are suspended at much smaller

gas velocity and distributed more uniformly in the bubble column with draught tube than in the column with flat bottom and without draught tube.

3) An empirical equation for U_c is proposed that is applicable to columns with diameter of 0.1–0.3 m.

Nomenclature

c	=	average solid concentration in gas-free slurry	$[kg \cdot m^{-3}]$
D_d	=	diameter of gas distributor	[m]
D_i	=	inner diameter of draught tube	[m]
D_{io}	=	D_i+2t_w, outer diameter of draught tube	[m]
D_o	=	column diameter	[m]
d_p	=	diameter of solid particle	[m]
g	=	gravitational acceleration	$[m \cdot s^{-2}]$
H	=	length of draught tube	[m]
H_L	=	static slurry height above gas distributor	[m]
L	=	vertical clearance between lower end of draught tube and wall of conical bottom shown in Fig. 2	[m]
n	=	number of pores in gas distributor	[—]
P_A	=	atmospheric pressure	[Pa]
P_s	=	$P_A+gH_L\{c+(\rho/\rho_p)(\rho_p-c)\}$, static pressure on gas distributor	[Pa]
ΔP_s	=	total pressure drop caused by suspended solids in liquid	[Pa]
Q_L	=	flow rate of bulk circulating liquid	$[m^3 \cdot s^{-1}]$
S_a	=	cross-sectional area of annulus	$[m^2]$
S_i	=	cross-sectional area of draught tube	$[m^2]$
S_o	=	cross-sectional area of column	$[m^2]$
T	=	temperature	[K]
t_w	=	wall thickness of draught tube	[m]
U_c	=	critical gas velocity based on cross section of column required for complete suspension of solid particles	$[m \cdot s^{-1}]$
U_G	=	gas velocity based on cross section of column and on static pressure P_s	$[m \cdot s^{-1}]$
U_{LC}	=	$8Q_L/\pi D_o^2$, average velocity of bulk circulating liquid flow	$[m \cdot s^{-1}]$
V_t	=	terminal velocity of a single particle in stagnant liquid	$[m \cdot s^{-1}]$
δ	=	diameter of holes in gas distributor	[m]
μ	=	liquid viscosity	[Pa·s]
σ	=	liquid density	$[kg \cdot m^{-3}]$
ρ_p	=	density of solid particle	$[kg \cdot m^{-3}]$
ρ	=	liquid surface tension	$[N \cdot m^{-1}]$

〈Subscripts〉

est.	=	estimated value
obs.	=	observed value

Literature Cited

1) Bohner, K. and H. Blenke: *Verfahrenstechnik*, **6**, 50 (1972).
2) Freedman, W. and J. F. Davidson: *Trans. Inst. Chem. Eng.*, **47**, T-251 (1969).
3) Gopal, J. S. and M. M. Sharma: *Can. J. Chem. Eng.*, **60**, 353 (1982).
4) Himmelblau, D. M.: "Process Analysis by Statistical Methods," p. 178, John Wiley & Sons (1970).
5) Kato, Y., A. Nishiwaki, T. Fukuda and S. Tanaka: *J. Chem. Eng. Japan*, **5**, 112 (1972).
6) Koide, K., T. Yasuda, S. Iwamoto and E. Fukuda: *J. Chem. Eng. Japan*, **16**, 7 (1983).
7) Koide, K., S. Iwamoto, Y. Takasaka, S. Matsuura, E. Takahashi, M. Kimura and H. Kubota: *J. Chem. Eng. Japan*, **17**, 459 (1984).
8) Lamont, A. G. W.: *Can. J. Chem. Eng.*, **31**, 153 (1958).
9) Matsuura, A., J. Ogawa and T. Akehata: Preprint of the Niigata Meeting of Soc. of Chem. Engrs., Japan, p. 61 (1982).
10) Muroyama, K., A. Yasunishi and Y. Mitani: Proceedings of the Third Pacific Chem. Eng. Congress, Vol. 1, p. 303 (1983).

(Presented in part at the Shinshu Meeting of The Society of Chemical Engineers, Japan, at Ueda, July 19, 1983.)